

Lifetime Improvement for Full-Width-Array Piezo Ink Jet Print Head Using Matrix Nozzle Arrangement

Shinji Seto, Takashi Yagi, Masakazu Okuda, Shigeru Umehara and Masaki Kataoka

New Marking Systems Laboratory, Corporate Research Group, Fuji Xerox Co., Ltd., 2274 Hongo, Ebina-shi,

Kanagawa 243-0494, Japan

E-mail: seto.shinji@fuji-xerox.co.jp

Abstract. Upon driving the unimorph type piezoelectric actuator of an ink jet in a high temperature high humidity environment (38°C/80%), many failures occurred after approximately 1 billion pulses. We hypothesized that the failures occurred due to hydrogen that was generated from the electrolysis of water, causing the piezoelectric element to deteriorate. Based on this hypothesis, we examined electrode materials to reduce the frequency of failures. We found that failure rate can be improved if material with high standard electrode potential is used as the electrode material on the high potential side and material with low standard electrode potential is used on the low potential side, and more specifically, if metal oxide is used for the electrode on the low potential side. Based on these findings, a combination of silver palladium for the electrode on the high potential side and stannous oxide (Sn_xO_y) for the low potential side was used as the combination of electrode materials that can be formed at low cost. Upon implementing a running test with this combination of electrode materials under a high temperature high humidity environment, we confirmed that failures do not occur even at a continuous drive of 30 billion pulses and that the long-term reliability of the unimorph type piezoelectric actuator improved significantly. © 2009 Society for Imaging Science and Technology. [DOI: 10.2352/J.ImagingSci.Technol.2009.53.5.050305]

INTRODUCTION

The development of full-width-array (FWA) ink jet units, which enables one-pass printing over the width of a paper, has been implemented for the purpose of speeding up ink jet printing.^{1,2} In recent years, the development of FWA ink jet units has been advancing rapidly with the improvement of manufacturing technology, which has achieved a steady increase in the number of nozzles in one ink jet head module.^{3–5} However, with the speeding up of printing, problems have become apparent such as the decrease in image quality due to smudges on the printed surface and blurring of ink onto the paper, which result from the slow drying of the ink. In order to solve these problems, the development of various types of ink is ongoing, e.g., high viscosity ink,⁶ ink sets that use two liquid reactants,⁷ and ink that is UV-curable. Since these types of inks use special media and solvents, there is a strong desire for the development of an ink jet head with wide ink latitude. In particular, ink jet head modules that use piezoelectric elements (Piezo ink jet head modules: PIJ head modules), where pressure is mechanically

applied to discharge ink, in principle, are suited for widening the ink latitude. There are expectations for the utility of these ink jet head modules in the use of discharging such highly functional ink. Furthermore, recently, PIJ head modules that use MEMS technology have been developed and put into practical use.⁸ This technology is utilized in the structural integration of flow paths in order to widen the ink latitude of PIJ head modules even further.

Up until now, the authors have been developing PIJ head modules with nozzles arranged in a matrix layout for the purpose of one-pass high-definition recording. The authors have now developed an FWA ink jet unit that has 7680 nozzles based on this technology. This FWA ink jet unit is configured with eight head modules that are connected to each other. In addition, high density of the nozzle arrangement has been realized by devising a configuration of the head modules, where the head modules are lined up in a single horizontal row in forming the FWA ink jet unit.

With the increase in the printing speed, demands for long-term reliability have increased more than ever. In this respect, we have conducted examinations on extending the operational life of piezoelectric actuators, in parallel with the development of the physical length-extension technology, which serves as the key in procuring long-term reliability of print heads. The piezoelectric actuator converts electric energy to mechanical energy and is the component that generates pressure for discharging ink. Since the piezoelectric actuator is subject to electrical, mechanical, and chemical stresses due to contact with the ink, it is subject to a multiple range of failure modes. For this reason, in order to improve the long-term reliability of the piezoelectric actuator, it is important to isolate each failure mode and to hypothesize the failure mechanism. It is at such a point where the failure modes were identified from the analysis of malfunctioned piezoelectric actuators and from verification experiments that the failure mechanism(s) could be hypothesized. In addition, improvement measures were established based on the hypothesized failure mechanism and the positive effects of such measures were confirmed.

STRUCTURES

Ejector

Figure 1 is a structural cross-section diagram of the ejector. The flow path section is comprised of a reservoir, ink supply

Received Jun. 25, 2008; accepted for publication Apr. 29, 2009; published online Aug. 26, 2009.

1062-3701/2009/53(5)/050305/7/\$20.00.

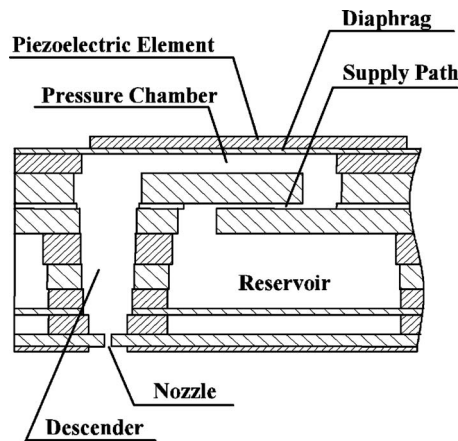


Figure 1. Cross section of an individual ejector.

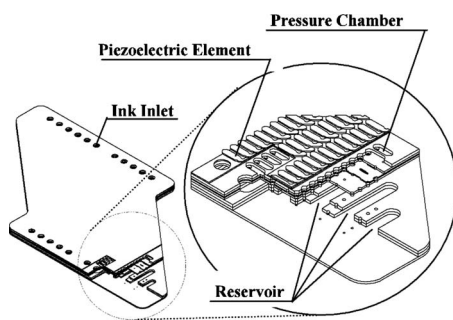


Figure 2. Oblique perspective diagram of stacking stainless steel plates. path, pressure chamber, and a connection path (“descender”) from the pressure chamber to the nozzle. This ejector is structured with nine laminated and joined stainless steel plates, which realize a highly ink-resistant flow path section at low cost. The actuator was created by forming electrodes, through sputtering, onto piezoelectric elements that were processed with wrap to a thickness of $35\ \mu\text{m}$, separating these elements for each ejector and bonding them onto a diaphragm (a “vibrating plate”) using an epoxy adhesive. This method of manufacturing an actuator is widely used as a method for forming highly efficient actuators at low costs.^{9,10}

Head Module

Figure 2 is a structural perspective diagram of the head unit (unit). With regard to the layout of the nozzles inside the unit, the ejector that was previously mentioned is arranged in a matrix layout so that there appears to be 600 nozzles/in. Figure 3 consists of a photo and computer-aided design image of the unit. Each unit has 1024 nozzles and the outside is structured as a schematic parallelogram. Each unit also has a flexible cable and an ink port, making jetting characteristic tests possible for each unit.

Full-width-array

Figure 4 is an external view of the long-length head unit that was created. As indicated in the diagram, eight PIJ head modules were arranged in a horizontal line and fixed to a single base material. This manufacturing method was used to create a long-length head unit with 7680 nozzles and a printable area of 12.8 in.

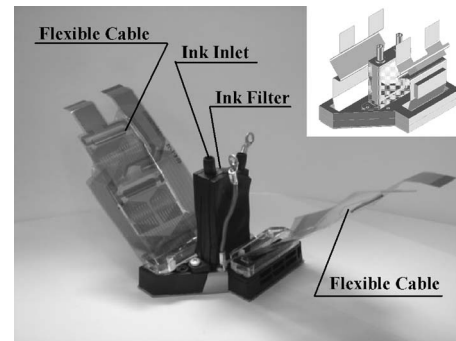


Figure 3. Photos and diagram of print head unit.

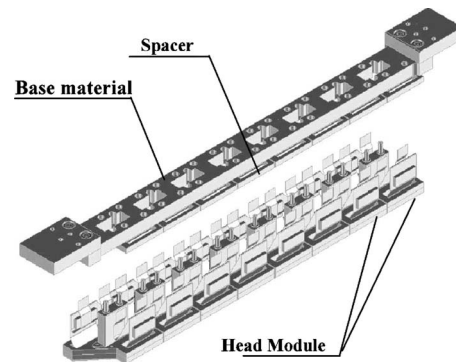


Figure 4. Oblique perspective diagram of full-width-array head.

The module was configured with a material for attachment and removal (“spacer”) inserted between the module and base material, so that the module could be easily removed from the base material. This configuration enables high accuracy when determining the position of the head module as well as the easy removal of the module from the base material. The positioning accuracy of the head module that was created was better than $\pm 9\ \mu\text{m}$ (3σ) by actual measurement.

The amount of thermal deformation is greater with a long-length head unit as compared to a short-length head unit, which poses a large problem. In a verification experiment in which both ends of the base material were fixed, the base material deformed greatly due to thermal change, resulting in a large displacement of the ink jetting position. This problem can be avoided by using material with a low thermal expansion coefficient as the base material, but such material is expensive. Consequently, a mechanism that absorbs thermal expansion and contraction was positioned on one side of the base material, and this was found to prevent deformation of the head unit.

KEY TO PERFORMANCE

Drop Formation

Figure 5 is an example of the state of jetting when the drive wave form has been modified. This PIJ head module is configured so that it is possible to select and apply drive wave forms to the piezoelectric element from among three types of drive wave forms per printing cycle. Accordingly, four-level gradation recording is realized.

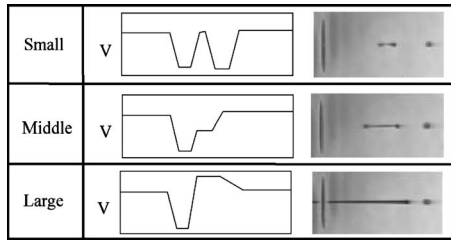


Figure 5. Jetting formation and driving wave form, from small volume to large volume at the same drop speed (10 m/s).

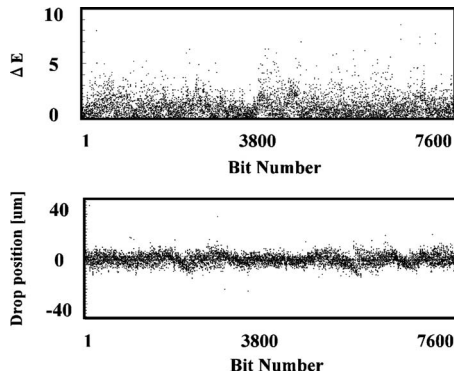


Figure 6. Color-difference and drop displacement in typical full-width-array at paper gap is 1.5 mm.

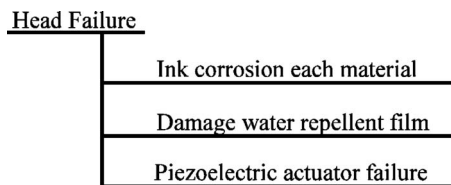


Figure 7. Classification of PJI heads failures.

Drop Uniformity

Figure 6 represents the measurement results for printing density and accuracy of the ink discharge position for the long-length head. In terms of uniformity of discharge, an average color difference (ΔE) of 1.2 and a drop displacement accuracy of approximately $\pm 15 \mu\text{m}$ (3σ) (when the gap between the head and paper sheet is 1.5 mm) were verified.

HEAD RELIABILITY

The items that influence the long-term reliability of piezo ink jet head modules are considered to be the three items shown in Figure 7. In this article, we report the improvement details with respect to the long-term reliability for piezoelectric actuators from among these items.

Failure Mode Classification

To identify the cause of piezoelectric actuator failure, the authors classified the failure modes as shown in Figure 8. First, the failure modes for the piezoelectric actuator were generally divided into two categories. The first is a mechanical mode that leads to failures resulting from physical stresses, such as stress concentration, and the second is a

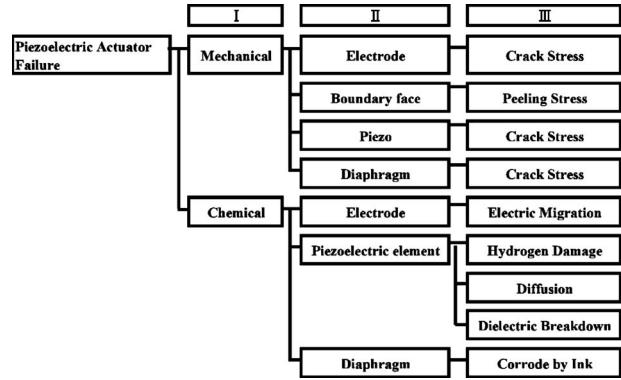


Figure 8. Classification of PA failure mode.

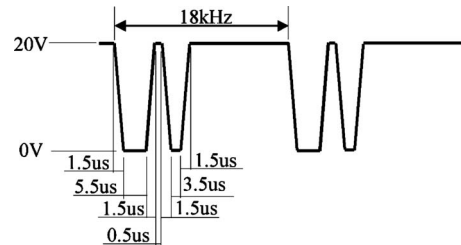


Figure 9. Driving wave form of the continuous drive test.

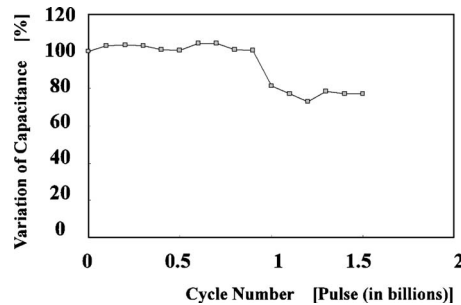


Figure 10. Result of continuous drive test under high temperature (38°C) and high humidity (80%).

chemical mode that is based on corrosion caused by the ink and electrochemical reactions. In addition, these two modes were further divided into nine modes according to failure location and failure contents.

Long-term Reliability Assessment Conditions

Figure 9 is a drive wave form that was used for assessing long-term reliability. This drive wave form was repetitiously applied at a frequency of 18 kHz in a high temperature (38°C) and high humidity (80%) environment. The piezoelectric element was polarized at a field intensity of 1 V/mm, and the field direction of the drive was the same as that during polarization.

Failure Mode Conclusion

Figure 10 shows the results of a continuous drive test. Since the change in the capacitance and the change in the displacement amount during the test demonstrated the same tendencies, only the change in the capacitance was indicated in this graph. At an applied pulse number of approximately 1

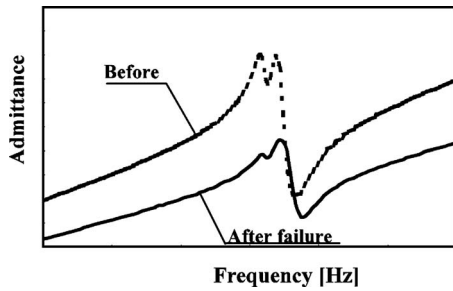


Figure 11. Admittance and phase of failure piezoelectric actuator before continuous drive test and after failure.

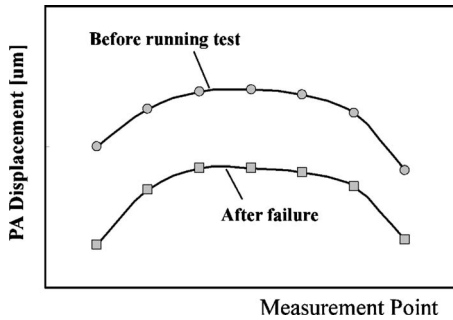


Figure 12. PA displacement of each point on piezoelectric actuator, before continuous drive test and after failure.

billion, the capacitance and displacement amount of the piezoelectric actuator decreased by 30% to 40%. Explanations based on the examination of the mechanism for this failure, the examination of improvement measures, and the results of the continuous drive test for the experimental product are presented below.

In order to improve failures, it is necessary to determine the failure modes and occurrence mechanisms and to establish improvement measures. As a result, an estimation of the failure modes based on the classifications for failure modes as shown in Fig. 8 was conducted.

First, the divisions for category I were reviewed. When damage to the piezoelectric element, damage to the diaphragm, or peeling of the interface occurs, the rigidity of the overall piezoelectric actuator decreases. Consequently, it is predicted that a decrease in the resonant frequency or a high frequency oscillation due to undamped vibrations will occur. Figure 11 shows the results of admittance measurement¹¹ before and after failure occurred. Based on the graph, it was

confirmed that the resonant frequency of the piezoelectric actuator (approximately 520 kHz) does not change much before and after the failure and that there were no vibrations of high frequency.

Figure 12 shows the results of measuring the piezoelectric actuator displacement amount before and after the failure at each point on the piezoelectric element’s upper surface. The displacement amount after the failure at each point decreased at nearly the same ratio as before failure, and there are no occurrences of abnormal vibration following the failure. Based on these results, it is considered that category I failures consisting of mechanical modes, such as the breakage of the piezoelectric element, breakage of the diaphragm, breakage of the electrode, and peeling of the adhesive material, do not occur—but rather—chemical modes are operative.

Next, category II items were isolated. Since the failure occurred even when ink was filled, it is not a result of corrosion of the diaphragm, based on the penetration of ink. Also, since the failure occurs even when electrochemically stable iridium (Ir) is used as the electrode material, the failure is not thought to be resulting from the migration of the electrode, and category II failures must comprise failures in the piezoelectric element section.

Last, category III was examined. Table I compares the piezoelectric actuator electric property values before and after the failure. The insulation resistance changes significantly before and after the failure and it can be confirmed that the failure is not caused by the insulation damage. In addition, since similar decreases in properties of IrO₂ electrodes, which are highly resistant to lead loss, were observed, this failure is not thought to result from the lead loss of the piezoelectric element. Based on the above results, it was judged that the failure is a chemical one resulting from hydrogen damage to the piezoelectric element section.

As mentioned above, a method of processing the piezoelectric element in order to make the element thinner combined with the adhesive bonding of the element onto a diaphragm is widely used and even commercialized. However, to the knowledge of the authors, there have been no reports of failures similar to what is described in this article. The cause behind the occurrence of the failure in this head module is thought to be the piezoarray structure. Specifically, since the nozzles of this head module are arranged in a matrix layout, the flexible cable leading to the piezoelectric

Table I. Changes in piezoelectric properties in a continuous drive test in a high temperature and high humidity environment.

		Sn _x O _y		Ir	
		Before	After	Before	After
Capacitance	pF	700	550	700	550
Dielectric loss	%	4	10	4	10
Resonance frequency	kHz	520	530	520	530
Insulating resistance	GΩ	≧100	≧100	≧100	≧100

Table II. Results of the continuous drive test upon changing the ambient room temperature.

		Temperature	
		10 °C	45 °C
Humidity	15%	0%	0%
	90%	1%	10%

element covers the entire surface of the piezoelectric element. It is thought that as a result moisture, which is the probable cause behind this failure, may become easily adhered to the piezoelectric element, leading to the failure that is unique to this head module.

Failure Mechanism Conclusion

As stated previously, to the knowledge of the authors, there have not been any reports on failures resulting from hydrogen damage to the piezoelectric element in the field of ink jet technology. However, many such incidents have been reported during Fe-random access memory (RAM) development.¹²⁻¹⁵ Among these, the generation of hydrogen that causes failures had often taken place during the manufacturing process. However, for this ink jet head module, there is no process where hydrogen is generated in the manufacturing process. Therefore, the generation of hydrogen is presumed to have occurred after the completion of the manufacturing process.

First, the process for the generation of hydrogen was examined and will be explained below. The following two characteristics were confirmed as conditions under which the failure occurs. The first characteristic is that there is an environmental dependence. Table II shows the results of the failure occurrence rate that were confirmed upon changing the ambient temperature and humidity. From the results, it was confirmed that this failure occurs often in a high temperature and high humidity environment and does not occur in a low temperature or low humidity environment. The second characteristic is the point that the failure does not occur with a nonoperating piezoelectric actuator, under any environmental circumstance. Based on these characteristics, we established a hypothesis where the generation of hydrogen occurs through moisture in the air adhering to a piezoelectric element and thereafter undergoing electrolysis.

Incidentally, the deterioration progresses gradually with conventional failures that result from fatigue. However, with this failure, the decrease in capacitance is sudden, roughly at a drive of 1 billion as indicated in Fig. 10. This phenomenon has been reported in failures arising as an effect of oxygen vacancy,¹⁵ and its mechanism has also been explained.¹⁶ Accordingly, in the failure described in this article, it is also expected that capacitance suddenly decreased.

Experiment

Based on the hypothesis for the failure mechanism, two measures for improving failures were examined as follows:

Measure 1: prevent adherence of moisture onto piezoelectric elements;

Measure 2: prevent electrolysis of moisture.

Measure 1 consists of a method for preventing adherence of moisture by either forming a low permeability coating on the piezoelectric element or by covering the piezoelectric element with low permeability material. However, higher costs are expected to be incurred with this measure.

As a result, an improvement measure based on measure 2 was examined. The authors considered that electrolysis of water could be prevented through a combination of piezoelectrode materials and reviewed combinations of electrode materials. Specifically, using the standard electrode potentials of the electrode materials as parameters, the authors created a sample with a change in materials combinations and reviewed electrode materials based on the results of a continuous drive test. Table III indicates that when Au is used for the electrode on the ground (GND) side, the occurrence of failures decreases, insofar as the standard electrode potential of the electrode on the anode side is higher, and that when IrO₂ is used for the electrode on the anode side, the occurrence of failures decreases, insofar as the standard electrode potential of the electrode on the GND side is lower.

Table III also shows that the failure occurrence rate improves even when Sn_xO_y is used on the anode side and IrO₂ is used on the GND side. As reported in documents related to Fe-RAM, this is thought to be due to metal oxides possessing a function for repairing oxygen vacancy resulting from hydrogen damage based on oxidation-reduction reactions. The authors then conducted repeated drives by shifting the orientation of the electric potential of the failed piezoelectric actuator to verify the effects of the repair based on the oxide electrode. Figure 13 shows the combination of

Table III. Failure ratio after running test under high-temp (38 °C) and high-humid (80%). Standard electrode potential: Au > IrO₂ > NbO_x > Sn_xO_y.

		High potential			
		Au	IrO ₂	NbO _x	Sn _x O _y
Ground	Au	10%	7%	36%	75%
	IrO ₂	-	3%	-	0%
	Sn _x O _y	-	0%	-	10%

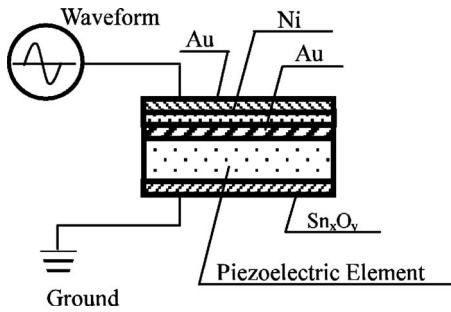


Figure 13. Configuration of electrode material on piezoelectric element with which confirmation of restoration was conducted.

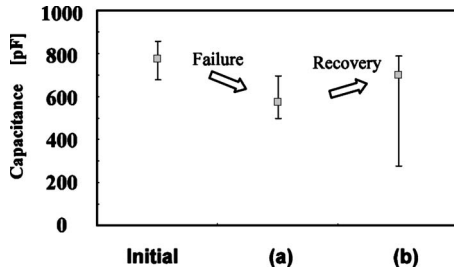


Figure 14. Results when reversing the direction of the electrical field and driving the failed piezoelectric actuator: (a) after continuous drive test in a high temperature, high humidity environment; (b) after continuous drive test when reversing the direction of the electrical field of failed head.

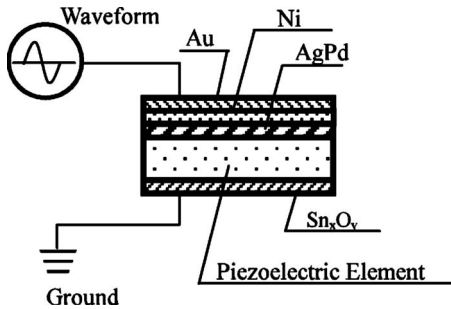


Figure 15. New electrode material over piezoelectric element.

electrodes that were used in the experiment. Figure 14 indicates that in many of the failed piezoelectric actuators, the capacitance becomes closer to the initial value before the failure. In other words, it is demonstrated that the piezoelectric element that received hydrogen damage is repaired by the Sn_xO_y electrode on the GND side.

Based on the above observations, it was inferred that by taking the standard electrode potential of the electrode into consideration, it becomes possible to control hydrogen damage and to realize a longer operating life.

Results of Run Test

Based on the results from the previous section, the electrode materials were selected as shown in Figure 15. Since the IrO_2 that was used in the verification experiment was an expensive material, silver palladium (AgPd), which is relatively inexpensive and has a high standard electric potential, was selected. For the GND side Sn_xO_y , which is a conductive oxide with a low standard electrode potential, was selected. With this electrode configuration, a continuous drive test

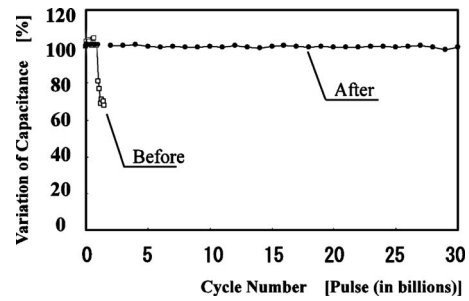


Figure 16. Result of continuous drive test under high temperature (38°C) and high humidity (80%) used new electrode material.

was implemented in a high temperature (38°C) and high humidity (80%) environment.

Figure 16 shows that there was a significant improvement in failures; whereas failures occurred at a level of approximately 1 billion pulses with the previous electrode configuration, failures did not occur even with a drive of 30 billion pulses, with the improved electrode configuration that was selected as a result of this research.

In this research, it was not possible to observe directly the state of deterioration of the piezoelectric element resulting from hydrogen damage. Although the authors were able to establish measures for improving the failures, whether or not hydrogen damage is really the cause is a matter for speculation.

SUMMARY

- (1) An FWA ink jet head unit with a print resolution 600×1200 dpi operating at printing speed of up to 90 pages per minute (ppm) that has 7680 nozzles for each color was created. Variation in characteristics inside the ink jet head unit was favorable, comprising only $\pm 15 \mu\text{m}$ (3σ) for discharge position accuracy, with an average color difference (ΔE) of 1.2.
- (2) Printing of 600×1200 dpi and 90 ppm was confirmed with the use of this ink jet head unit.
- (3) By changing the electrode configuration of piezoelectric element to AgPd/ Sn_xO_y , a longer operating life for piezoelectric actuators (no failures with 30 billion dots) in a high temperature and high humidity environment was achieved.

In this article, a method was explained for improving failures as a long-term reliable technology, but a separate examination of a method for tolerating failures is ongoing.¹⁷ In the future, we anticipate that ink jet technology will become widespread in the printing market through the development of an ink jet system that combines these technologies, achieving further high reliability in maintaining image quality.

REFERENCES

¹T. Hara, "Bubble jet recording", Journal of the Institute of Image Electronics Engineers of Japan 11, 66–71 (1982).
²N. Morita, "Multinozzle drop generator for continuous ink jet printing",

- Electronics and Communication in Japan, Part 2 **72**, 78–86 (1989).
- ³C. Tanuma, “Technical trends in ink jet printheads for industrial applications”, *Journal of the Imaging Society of Japan* **43**, 82–88 (2004).
- ⁴K. Silverbrook, “A 1600 npi pagewidth ink jet technology which features cost competitiveness with scanning ink jet: Home, office, and wide format applications”, *80th Global IJP Conference* (2007).
- ⁵S. Ishikura and A. Matsumoto, “Improvement in printing throughput for piezoelectric line ink jet print head,” *Proc. IS&T’s NIP23* (IS&T, Springfield, VA, 2007), pp. 305–330.
- ⁶Y. Ohta, “GELJET printer IPSiO G707/G505”, *Proc. ICJ* (Imaging Society of Japan, Tokyo, 2004).
- ⁷T. Doi, K. Yamashita, M. Numata, and K. Hashimoto, “Novel aqueous ink jet ink technology realizing high image quality and high print speed”, *Proc. IS&T’s NIP23* (IS&T, Springfield, VA, 2007), pp. 95–98.
- ⁸W. Letendre, S. Halwawala, and B. Smith, “Jetting and imaging performance of the M-300/10 jet module”, *Proc. IS&T’s NIP22* (IS&T, Springfield, VA, 2006).
- ⁹A. Bibl, Z. Chen, and J. Birkmeyer, “Print head with thin membrane”, US Patent Appl. 2005/0099467 A1 (2005).
- ¹⁰T. Yasuhara and K. Matsumoto, “Ink jet printing head”, US Patent 4,937,597 (1990).
- ¹¹T. Wada, H. Nakamura, and S. Hirakata, “Evaluation of ejecting drops on PIJ head by using Mahalanobis distance”, *Proc. ICJ* (Imaging Society of Japan, Tokyo, 2007), pp. 129–132.
- ¹²Y. Shinomoto, K. Kushida-Abdelghafar, H. Miki, and Y. Fujisaki, “H₂ damage of ferroelectric Pb(Zr,Ti)O₃ thin-film capacitors: The role of catalytic and adsorptive activity of the top electrode”, *Appl. Phys. Lett.* **70**, 3096 (1997).
- ¹³N. Ikarashi, “Analytical transmission electron microscopy of hydrogen-induced degradation in ferroelectric Pb(Zr,Ti)O₃ on Pt electrode”, *Appl. Phys. Lett.* **73**, 1955 (1998).
- ¹⁴S. Aggarwal, “Recovery of forming gas damaged Pb(Nb,Zr,Ti)O₃ capacitors”, *Appl. Phys. Lett.* **76**, 918–920 (2000).
- ¹⁵Dong-Chun Kim and Won-Jong Lee, “Effect of LaNiO₃ top electrode on the resistance of Pb(Zr,Ti)O₃ ferroelectric capacitor to hydrogen damage and fatigue”, *Jpn. J. Appl. Phys.* **41**, 1470–1476 (2002).
- ¹⁶J. F. Scott, “A model for fatigue in ferroelectric perovskite thin films”, *Appl. Phys. Lett.* **76**, 3801 (2000).
- ¹⁷D. Tatsumi and T. Shimizu, “A white streak reduction method by error diffusion”, *Proc. ICJ* (Imaging Society of Japan, Tokyo, 2007), pp. 141–144.